

Spectral dynamics of incoherent waves with a noninstantaneous nonlinear response

Gang Xu,^{1,*} Josselin Garnier,² Stefano Trillo,³ and Antonio Picozzi¹

¹Laboratoire Interdisciplinaire Carnot de Bourgogne (ICB), CNRS - University of Burgundy, Dijon, France

²Laboratoire de Probabilités et Modèles Aléatoires, University Paris Diderot, 75205 Paris Cedex 13, France

³Department of Engineering, University of Ferrara, Via Saragat 1, 44122 Ferrara, Italy

*Corresponding author: gang.xu@u-bourgogne.fr

Received May 24, 2013; revised July 3, 2013; accepted July 13, 2013;

posted July 15, 2013 (Doc. ID 191132); published August 5, 2013

We study the influence of a constant background noise on the dynamics of spectral incoherent solitons, which are incoherent structures sustained by a noninstantaneous (Raman-like) nonlinearity. As the level of the noise background increases, the incoherent wave enters a novel nonlinear regime characterized by oscillatory dynamics of the incoherent spectrum, which develop within a spectral cone during the propagation. In contrast to the conventional Raman-like spectral red shift, such incoherent spectral dynamics can be characterized by a significant spectral blue shift. On the basis of the kinetic wave theory, we derive explicit analytical expressions of these incoherent oscillatory spectral dynamics. © 2013 Optical Society of America

OCIS codes: (190.4370) Nonlinear optics, fibers; (190.5650) Raman effect; (030.1640) Coherence.

<http://dx.doi.org/10.1364/OL.38.002972>

The propagation of partially coherent nonlinear optical waves is a subject of growing interest in different fields of investigations, such as, e.g., wave propagation in homogeneous [1–5] or periodic media [6], waveguides [7], cavity systems [8–15], supercontinuum (SC) generation [16–18], or nonlinear interferometry [19,20]. When the propagation of the incoherent optical wave is essentially conservative (i.e., ruled by a Hamiltonian equation), its long-term evolution should be characterized by a non-equilibrium process of thermalization. In analogy with the kinetics of a gas system, wave thermalization manifests itself by means of an irreversible evolution of the optical field toward the thermodynamic equilibrium state (maximum of entropy) [21].

A fundamental problem is to understand the physical processes that can inhibit this natural phenomenon of optical wave thermalization. Different mechanisms have been identified in recent years, e.g., the presence of a highly nonlocal nonlinearity [22] or the existence of additional invariants in the 1D nonlinear Schrödinger equation (NLSE) [23–27]. In particular, the presence of a noninstantaneous response of the nonlinear medium breaks the conservative (Hamiltonian) nature of wave propagation, which in turn prevents the irreversible process of thermalization [21]. A typical example is provided by the Raman effect in optical fibers. In this case the incoherent wave has been shown to self-organize into spectral incoherent solitons (SISs), i.e., incoherent solitons that cannot be identified in the spatio-temporal domain but solely in the spectral domain [28–31]. The origin of SISs relies on the causality property inherent to the delayed nonlinear response function: as a result of the antisymmetric (Raman) gain spectrum, the low-frequency components of SISs are amplified to the detriment of their high-frequency components, thus leading to a permanent spectral red shift of SISs [28–30].

Our aim in this Letter is to show that such dynamics of incoherent waves change in a dramatic way in the presence of a constant spectral background noise. Instead of the expected SIS-like behavior, we show that the

incoherent wave enters a novel regime: it is characterized by oscillatory dynamics of the incoherent spectrum that develop within a spectral cone during propagation. The remarkable and unexpected result is that such spectral dynamics exhibit a significant spectral blue shift, which is in marked contrast with the usual Raman-like spectral red shift. A wave turbulence approach of the problem provides a detailed description of these incoherent oscillatory dynamics: we obtain explicit analytical expressions for the spectral evolution of the incoherent wave, which are in quantitative agreement with the simulations of the NLSE without adjustable parameters.

Besides its fundamental interest, this novel regime of incoherent wave propagation can shed new light on the spectral dynamics of incoherent waves superimposed on an incoherent SC spectral background. More generally, optical fibers and waveguides [32] turn out to be ideal test beds for experimental verification of our predictions, thanks to the easily tailorable Raman response function, as well as other recently investigated mechanisms involving liquid cores or photoionizable noble gases and surface plasmon polaritons [33–36].

We consider the standard NLSE accounting for a non-instantaneous Kerr effect

$$i\partial_z A - \beta\partial_{tt} A + \gamma A \int R(t-t')|A|^2(z,t')dt' = 0, \quad (1)$$

where the response function $R(t)$ is constrained by the causality condition, $R(t) = 0$ for $t < 0$. γ is the nonlinear Kerr coefficient, while $\beta = (1/2)\partial_{\omega}^2 k|_{\omega_0}$ refers to the second-order dispersion coefficient [31]. The nonlinear length is defined as $L_{\text{nl}} = 1/(\gamma P)$, where P is the average power of the incoherent wave. The typical width of $R(t)$, say τ_R , denotes the response time of the nonlinearity. As previously discussed [21,37], the dynamics is ruled by the comparison of τ_R with the “healing time,” $\tau_0 = \sqrt{|\beta|L_{\text{nl}}}$, which denotes the typical modulational instability period in the limit of an instantaneous response $\tau_R \rightarrow 0$. In the

following we consider the standard regime $\tau_R \sim \tau_0$, which leads in particular to the generation of SISs.

We report in Fig. 1 the evolution of the spectrum of the incoherent wave obtained by integrating numerically the NLSE (1). We considered the Raman response function, $R(t) = H(t) \left[1 + \alpha^2 / (\alpha \tau_R) \right] \sin(\alpha t / \tau_R) \exp(-t / \tau_R)$, with $\tau_R = 32$ fs and $\alpha = \tau_R / \tau_1 \simeq 2.6$ ($\tau_1 = 12.2$ fs), and $H(t)$ denotes the Heaviside function [31]. The initial condition is a partially coherent wave with a Gaussian spectrum and random spectral phases, superimposed on a white noise spectral background. The initial Gaussian spectral width is of the same order as the spectral bandwidth of the gain spectrum, which refers to the imaginary part of the Fourier transform of the response function, $g(\omega) = \Im[\tilde{R}(\omega)]$. The amount of spectral noise background is simply defined from the ratio, say ρ , between the background noise level and the amplitude of the initial Gaussian spectrum. In the presence of a small-amplitude background noise ($\rho \ll 1$), the incoherent wave rapidly evolves into an SIS, which is red shifted with a constant velocity in frequency space [28–30]. However, as the noise background level increases and becomes of the same order as the initial Gaussian hump (i.e., $\rho \geq 1$), the dynamics enters a novel regime: the incoherent spectrum exhibits oscillatory behavior, which spreads during the propagation along a spectral cone with both red and blue spectral shifts [see Fig. 1(c)].

In order to describe the properties of this regime, we resort to a statistical description of the random field based on the wave turbulence theory [38]. Assuming that the weakly nonlinear random wave exhibits stationary statistics, one obtains a natural closure of the hierarchy of moments equations [21]: the averaged spectrum of the wave, $n_\omega(z) = \int B(z, \tau) \exp(-i\omega\tau) d\tau$, where $B(z, \tau) = \langle A(z, t - \tau/2) A^*(z, t + \tau/2) \rangle$ is the correlation function, evolves according to the kinetic equation (KE)

$$\partial_z n_\omega = \frac{\gamma}{\pi} n_\omega \int_{-\infty}^{+\infty} g(\omega - \omega') n_{\omega'} d\omega'. \quad (2)$$

This KE has been shown to provide a detailed deterministic description of the properties of SISs in different physical conditions [28–30]. To study the new incoherent oscillatory dynamics, we pose $n(\omega, z) = n_0 + \tilde{n}(\omega, z)$, where $n_0 (\gg \tilde{n}_\omega)$ denotes the background noise level [$\rho = n_0 / \tilde{n}_{\omega=0}(z=0)$]. Keeping in mind that $g(\omega)$ is odd, the KE (2) gets linearized $\partial_z \tilde{n}_\omega = (\gamma/\pi) n_0 \int_{-\infty}^{+\infty} g(\omega - \omega') \tilde{n}_{\omega'} d\omega'$. Its solution can be written by defining $\tilde{B}(t, z) = (1/2\pi) \int_{-\infty}^{+\infty} \tilde{n}_\omega(z) \exp(i\omega t) d\omega$ and $G(t) = (i/2\pi) \int_{-\infty}^{+\infty} g(\omega) \exp(i\omega t) d\omega$, where the function $G(t)$ is real and odd. The general solution thus reads

$$\tilde{n}_\omega(z) = \int_{-\infty}^{+\infty} \tilde{B}_0(t) \exp[-2i\gamma n_0 G(t)z - i\omega t] dt, \quad (3)$$

where $\tilde{B}_0(t) = \tilde{B}(t, z=0)$. Assuming furthermore that $\tilde{B}_0(t)$ is even and real, and remarking that $G(t) = (1/2)[R(t) - R(-t)]$, the solution (3) takes the form

$$\tilde{n}_\omega(z) = 2 \int_0^\infty \tilde{B}_0(t) \cos[\gamma n_0 R(t)z + \omega t] dt. \quad (4)$$

Making use of the stationary phase method, one can derive an explicit analytical solution for $\tilde{n}_\omega(z)$ in the limit $\gamma n_0 z \max_{t>0}(|R|(t)) \gg 1$. It is important to underline that *the condition for the existence of the stationary critical point determines the properties of the cone of incoherent spectral oscillations* [see Figs. 1(c) and 1(d)]. Indeed, a stationary critical point of Eq. (4), say t_j , is determined by the solution of the equation $\varphi'(t_j) = 0$, where $\varphi(t) = \gamma n_0 R(t)z + \omega t$, i.e., $\gamma n_0 R'(t_j) = -\omega/z$, where $R'(t) = \partial_t R(t)$, and $\varphi'(t) = \partial_t \varphi(t)$. It turns out that $t_j = f(\omega/z)$ is a function of ω/z . This reveals that the evolution of $\tilde{n}_\omega(z)$ is essentially bounded on a spectral cone defined by the frequency interval $\omega \in [\omega_{\min}, \omega_{\max}]$:

$$\omega_{\min} = \gamma n_0 z \min_{t>0}(-R'(t)), \quad (5)$$

$$\omega_{\max} = \gamma n_0 z \max_{t>0}(-R'(t)). \quad (6)$$

According to the stationary phase method, the solution $\tilde{n}_\omega(z)$ is of order $1/\sqrt{z}$ in this interval.

We illustrate this behavior by considering different concrete examples. We start with the purely exponential response function, $R(t) = H(t) \exp(-t/\tau_R)/\tau_R$, which is known to model a noninstantaneous Kerr nonlinearity [33] (also see metal-based surface plasmonic devices [36]). As illustrated in Fig. 2(a), we have in this case a single critical point, $t_1(\omega/z) = \tau_R \log[\gamma n_0 z / (\omega \tau_R^2)]$. According to the stationary phase method, the solution to Eq. (4) reads for $\omega \in [\omega_{\min}, \omega_{\max}]$

$$\tilde{n}_\omega(z) \simeq \frac{2\sqrt{2\pi\tau_R}\tilde{B}_0(t_1(\omega/z))}{\sqrt{z}\sqrt{|\omega/z|}} \cos[K(\omega/z)z + \pi/4], \quad (7)$$

where

$$K(\omega/z) = \tau_R [1 + \log(\gamma n_0 z / (\omega \tau_R^2))] \omega/z. \quad (8)$$

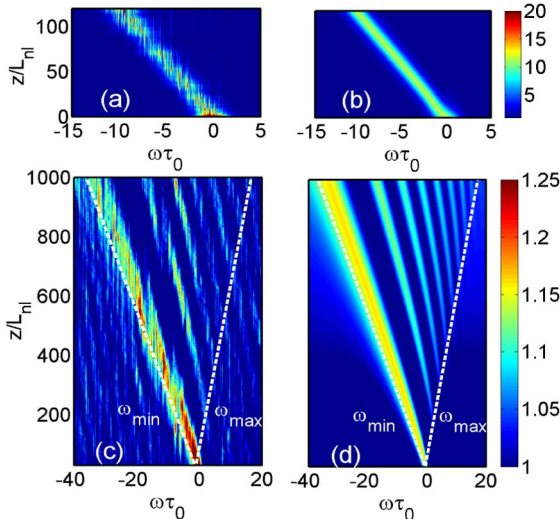


Fig. 1. Simulations of (a), (c) NLSE (1) and (b), (d) kinetic equation (2) for the damped harmonic oscillator (Raman-like) response. As the level of the background noise increases [(a), (b) $\rho = 0.1$; (c), (d) $\rho = 3$], the incoherent wave exhibits a transition from the SIS regime (a), (b), to the new regime characterized by oscillations that develop within a spectral cone (c), (d) ($\tau_R = 2.5\tau_0$).

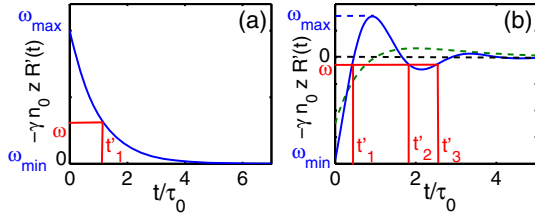


Fig. 2. (a) Schematic representation of the derivative of the response function for the exponential response, (b) damped harmonic oscillator response for $\alpha = 0$ (dashed green), $\alpha = 2.6$ (solid blue), and the corresponding values of ω_{\min} and ω_{\max} [see Eqs. (5) and (6)]. Note that t'_j denotes t_j/τ_0 ($j = 1, 2, 3$).

Quite remarkably, in this case *the spectrum experiences a pure spectral blue shift*, since $\omega_{\min} = 0$ and $\omega_{\max} = \gamma n_0 z / \tau_R^2$ [see Fig. 2(a)]. This unexpected prediction has been confirmed by the numerical simulations of the NLSE and KE, as remarkably illustrated in Fig. 3. Quantitative agreement has been obtained between the simulations and the plot of the analytical solution [Eqs. (7) and (8)], without adjustable parameters. We remark that this spectral blue shift is of a fundamentally different nature than those recently discussed in [34,35].

We now consider the example of the damped harmonic oscillator response discussed above through Fig. 1. In this case we have $\omega_{\min} = -\gamma n_0 z (1 + \alpha^2) / \tau_R^2$, and

$$\omega_{\max} = \frac{\gamma n_0 z}{\tau_R^2} (1 + \alpha^2) \exp \left[-\alpha^{-1} \left(\operatorname{atan} \left(\frac{2\alpha}{1 - \alpha^2} \right) + \sigma \pi \right) \right], \quad (9)$$

where $\sigma = 0$ for $\alpha < 1$ and $\sigma = +1$ for $\alpha > 1$. Because of the oscillatory nature of $R(t)$, several critical points $t_j(\omega/z)$ contribute to the solution of Eq. (4), so that the general solution reads

$$\tilde{n}_\omega(z) \simeq \sum_{j=1}^m \frac{2\sqrt{2\pi} \tilde{B}_0(t_j(\omega/z))}{\sqrt{\gamma |R''(t_j(\omega/z))| n_0 z}} \cos[\Theta_j(\omega, z)], \quad (10)$$

where $\Theta_j(\omega, z) = K_j(\omega/z)z + s_j\pi/4$, with $s_j = \operatorname{sign}(R''(t_j))$ and

$$K_j(\omega/z) = \gamma n_0 R(t_j(\omega/z)) + t_j(\omega/z)\omega/z. \quad (11)$$

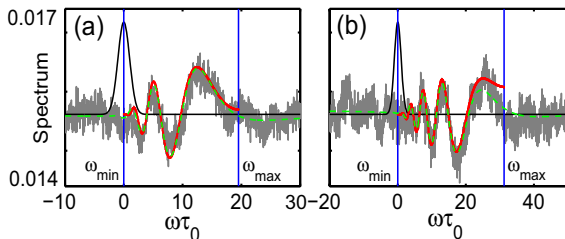


Fig. 3. Simulations of the NLSE (1) (gray) and KE (2) (green) for the exponential response function (the solid black line denotes the initial condition). The incoherent wave exhibits a spectral *blue shift*, instead of the expected red shift. Plot of the analytical solution given in Eqs. (7) and (8) (red). Quantitative agreement is obtained between the analytical solution and the simulations of the NLSE and KE [(a) $z = 1250L_{\text{nl}}$; (b) $z = 2000L_{\text{nl}}$]; $\tau_R = \tau_0 = 32$ fs, $\rho = 10$. The vertical lines denote the analytical expressions of $\omega_{\min, \max}$ given in the text.

We first comment on this general solution in the limit $\alpha \rightarrow 0$ [see Fig. 2(b), green line]. In this case we have for $\omega \in [\omega_{\min}, 0]$ a single contribution to the sum (10), i.e., $m = 1$ and $s_1 = -1$, where $t_1(\omega/z) < \tau_R$ verifies $\exp(-t_1/\tau_R)(1 - t_1/\tau_R) = -\tau_R^2 \omega / (\gamma n_0 z)$. For $\omega \in [0, \omega_{\max}]$ we have two contributions to the sum (10), with $\tau_R < t_1 < 2\tau_R$ ($s_1 = -1$) and $t_2 > 2\tau_R$ ($s_2 = +1$).

As the parameter α increases, one obtains many contributions to the sum (10), as schematically illustrated in Fig. 2(b). The general solution can thus be plotted by computing numerically the functions $t_j(\omega/z)$ solutions of $R'(t_j) = -\omega / (\gamma n_0 z)$. Quantitative agreement between the solution (10) and (11) and the numerical simulations of the NLSE (1) and KE (2) is obtained, without using adjustable parameters. This is remarkably illustrated in Fig. 4 for $\alpha = 0$ [Figs. 4(a) and 4(b)], and $\alpha = 2.6$ [Figs. 4(c) and 4(d)]. It is interesting to note that for $\alpha = 2.6$, the averaged spectrum $\tilde{n}_\omega(z)$ exhibits rapid and irregular oscillations, which result from the multiple oscillating contributions to the sum involved in the solution (10) and (11). Note that a temporal beating associated with such incoherent spectral oscillations cannot be identified in the temporal domain, in which the field exhibits stationary statistics [see Figs. 4(e) and 4(f)]. Finally, we remark that the predictions of Figs. 4(c) and 4(d) can be observed in a standard photonic crystal fiber, e.g., with $\beta_2 = 10^{-26}$ s²/m, $\gamma = 0.1$ W⁻¹ m⁻¹, and a power of ~ 100 W. Figure 4(c) would thus correspond to a propagation length of 30 m and a spectral blue shift of 72 THz.

The theoretical analysis reported here is general and can be applied to any specific form of the response function $R(t)$. For instance, the design and development of subwavelength photonic devices with metallic components has become a subject of intense research. We have extended our work by considering the two-temperature model underlying the response of surface plasmon polaritons in metal nanowires [36]. Our results confirm the existence of the novel nonlinear regime of incoherent spectral oscillations in metal-based plasmonic devices.

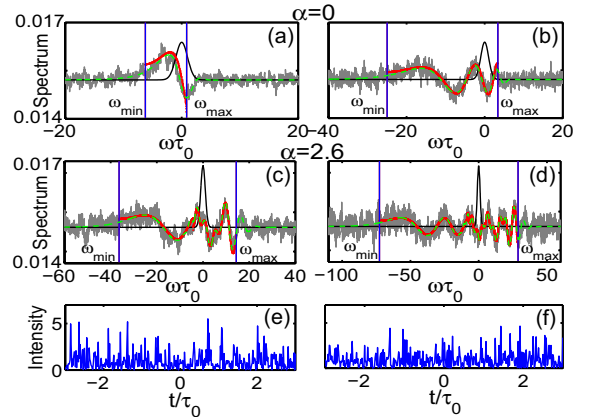


Fig. 4. Simulations of the NLSE (gray) and KE (green) for the damped harmonic oscillator response: (a), (b) $\alpha = 0$; (c), (d) $\alpha = 2.6$ (the solid black line denotes the initial condition). Quantitative agreement is obtained between the analytical solution [Eq. (7), red] and the simulations of the NLSE and KE [(a) $z = 400$, (b) $z = 1600$, (c) $z = 300$, (d) $z = 600$, in units of L_{nl}]; $\tau_R = \tau_0 = 32$ fs, $\rho = 10$. (e) Typical intensity profiles $|A|^2(t)$ corresponding to the spectra (c), (d).

ST acknowledges support from iXCore Foundation and MIUR (grant PRIN 2009P3K72Z). This work has been supported by the Labex ACTION program (contract ANR-11-LABX-01-01).

References

1. A. Fratalocchi, C. Conti, G. Ruocco, and S. Trillo, *Phys. Rev. Lett.* **101**, 044101 (2008).
2. D. Dylov and J. Fleischer, in *Localized States in Physics: Solitons and Patterns*, Part 1 (Springer, 2011), pp. 17–34.
3. A. Picozzi and P. Aschieri, *Phys. Rev. E* **72**, 046606 (2005).
4. A. Piskarskas, V. Pyragaite, and A. Stabinis, *Phys. Rev. A* **82**, 053817 (2010).
5. J. Laurie, U. Bortolozzo, S. Nazarenko, and S. Residori, *Phys. Rep.* **514**, 121 (2012).
6. Y. Silberberg, Y. Lahini, E. Small, and R. Morandotti, *Phys. Rev. Lett.* **102**, 233904 (2009).
7. P. Aschieri, J. Garnier, C. Michel, V. Doya, and A. Picozzi, *Phys. Rev. A* **83**, 033838 (2011).
8. C. Conti, M. Leonetti, A. Fratalocchi, L. Angelani, and G. Ruocco, *Phys. Rev. Lett.* **101**, 143901 (2008).
9. S. Babin, D. Churkin, A. Ismagulov, S. Kablukov, and E. Podivilov, *J. Opt. Soc. Am. B* **24**, 1729 (2007).
10. E. G. Turitsyna, G. Falkovich, V. K. Mezentsev, and S. K. Turitsyn, *Phys. Rev. A* **80**, 031804 (2009).
11. E. G. Turitsyna, G. Falkovich, A. El-Taher, X. Shu, P. Harper, and S. K. Turitsyn, *Proc. R. Soc. A* **468**, 2496 (2012).
12. R. Weill, B. Fischer, and O. Gat, *Phys. Rev. Lett.* **104**, 173901 (2010).
13. A. Schwartz and B. Fischer, *Opt. Express* **21**, 6196 (2013).
14. A. Schwache and F. Mitschke, *Phys. Rev. E* **55**, 7720 (1997).
15. S. Kobtsev, S. Kukarin, S. Smirnov, S. Turitsyn, and A. Latkin, *Opt. Express* **17**, 20707 (2009).
16. B. Barviau, B. Kibler, A. Kudlinski, A. Mussot, G. Millot, and A. Picozzi, *Opt. Express* **17**, 7392 (2009).
17. B. Barviau, B. Kibler, and A. Picozzi, *Phys. Rev. A* **79**, 063840 (2009).
18. M. Erkintalo, M. Surakka, J. Turunen, A. T. Friberg, and G. Genty, *Opt. Lett.* **37**, 169 (2012).
19. Y. Bromberg, Y. Lahini, E. Small, and Y. Silberberg, *Nat. Photonics* **4**, 721 (2010).
20. S. Derevyanko and E. Small, *Phys. Rev. A* **85**, 053816 (2012).
21. J. Garnier, M. Lisak, and A. Picozzi, *J. Opt. Soc. Am. B* **29**, 2229 (2012).
22. A. Picozzi and J. Garnier, *Phys. Rev. Lett.* **107**, 233901 (2011).
23. D. B. Soh, J. P. Kopolow, S. W. Moore, K. L. Schroder, and W. L. Hsu, *Opt. Express* **18**, 22393 (2010).
24. P. Suret, A. Picozzi, and S. Randoux, *Opt. Express* **19**, 17852 (2011).
25. P. Suret, S. Randoux, H. R. Jauslin, and A. Picozzi, *Phys. Rev. Lett.* **104**, 054101 (2010).
26. C. Michel, P. Suret, S. Randoux, H. R. Jauslin, and A. Picozzi, *Opt. Lett.* **35**, 2367 (2010).
27. B. Barviau, J. Garnier, G. Xu, B. Kibler, G. Millot, and A. Picozzi, *Phys. Rev. A* **87**, 035803 (2013).
28. A. Picozzi, S. Pitois, and G. Millot, *Phys. Rev. Lett.* **101**, 093901 (2008).
29. C. Michel, B. Kibler, and A. Picozzi, *Phys. Rev. A* **83**, 023806 (2011).
30. B. Kibler, C. Michel, A. Kudlinski, B. Barviau, G. Millot, and A. Picozzi, *Phys. Rev. E* **84**, 066605 (2011).
31. G. P. Agrawal, *Nonlinear Fiber Optics*, 5th ed. (Academic, 2012).
32. G. Fanjoux, J. Michaud, H. Maillotte, and T. Sylvestre, *Phys. Rev. Lett.* **100**, 013908 (2008).
33. C. Conti, M. A. Schmidt, P. St. J. Russell, and F. Biancalana, *Phys. Rev. Lett.* **105**, 263902 (2010).
34. M. F. Saleh, W. Chang, P. Hölzer, A. Nazarkin, J. C. Travers, N. Y. Joly, P. St. J. Russell, and F. Biancalana, *Phys. Rev. Lett.* **107**, 203902 (2011).
35. C. A. Husko, S. Combrie, P. Colman, J. Zheng, A. de Rossi, and C. W. Wong, *Nature Sci. Rep.* **3**, 1100 (2013).
36. A. Marini, M. Conforti, G. Della Valle, H. W. Lee, T. X. Tran, W. Chang, M. A. Schmidt, S. Longhi, P. St. J. Russell, and F. Biancalana, *New J. Phys.* **15**, 013033 (2013).
37. B. Kibler, C. Michel, J. Garnier, and A. Picozzi, *Opt. Lett.* **37**, 2472 (2012).
38. S. L. Musher, A. M. Rubenchik, and V. E. Zakharov, *Phys. Rep.* **252**, 177 (1995).